

Self-Oscillations of Large-Scale Circulation Intensity in the Black Sea

A. A. Pavlushin

Marine Hydrophysical Institute of RAS, Sevastopol, Russian Federation

✉ pavlushin@mhi-ras.ru

Abstract

Purpose. The work is aimed at investigating the influence of seasonal variability of tangential wind stress vorticity on the features of formation and intensity of the large-scale circulation in the Black Sea using the numerical simulation method.

Methods and Results. Numerical experiments within the framework of the two-layer eddy-resolving model of the Black Sea were carried with the sea surface subjected to a periodical seasonally changing field of tangential wind stress, the average annual intensity of which was constant during one individual experiment, but was various in different experiments. Numerical integration over time was performed for a long time period, which was sufficient for the model solution to be considered statistically equilibrium. The large-scale circulation intensity was determined from the integral values of the model energy characteristics, namely the kinetic and available potential energies. The calculations have resulted in the long-term series of instantaneous current fields in the two-layer sea at different wind forcing intensity, which were subjected to further analysis.

Conclusions. It has been established that in the Black Sea at certain parameters of wind forcing, the fluctuations can be induced in the large-scale circulation intensity with a period 6–8 years; at that the interannual variability of the average annual value of the tangential wind stress vorticity is not a reason of this phenomena. Taking into account the fact that the exciting wind forcing in the performed experiments was only of seasonal variability and repeated from year to year, the model-obtained long-term fluctuations in the large-scale currents intensity could be classified as the self-oscillations. The latter are the non-damped oscillations supported by an external energy source, the supply of which is regulated by the oscillatory system itself. In the case under consideration, the feedback mechanism required for the existence of self-oscillations, is provided by the dependence of the wind energy flow entering the sea upon the spatial distribution of surface currents, which can change in consequence of hydrodynamic instability of the currents and generation of the Rossby waves.

Keywords: Black Sea, large-scale circulation intensity, interannual variability, self-oscillations, baroclinic Rossby waves

Acknowledgements: The study was carried out within the framework of the state assignment of the MHI RAS on theme FNNN-2021-0003 “Development of operational oceanology methods based on interdisciplinary research of the processes of marine environment formation and evolution, and mathematical modeling using the data of remote and contact measurements”.

For citation: Pavlushin, A. A., 2022. Self-Oscillations of Large-Scale Circulation Intensity in the Black Sea. *Physical Oceanography*, 29(6), pp. 587-601. doi:10.22449/1573-160X-2022-6-587-601

DOI: 10.22449/1573-160X-2022-6-587-601

© A. A. Pavlushin, 2022

© Physical Oceanography, 2022

Introduction

Based on the observations and reanalysis data [1–5], the large-scale circulation intensity in the Black Sea undergoes significant seasonal and interannual changes. The main reason given for this is the variability of external conditions that determine the very existence of a large-scale cyclonic circulation in the Black Sea, namely, the integral vorticity of the tangential wind stress, having a cyclonic character on average over the entire sea area [6–8].



The present paper is aimed at a simplified hydrodynamic model usage to test the correctness of existing hypotheses about the causes of oscillations in the large-scale circulation intensity in the Black Sea and at trying to understand the physical mechanisms of this phenomenon. As a criterion for the large-scale circulation intensity, the values of the kinetic and available potential energies averaged over the sea area, which are easily determined from the simulation results, are used.

The model parameters and description of the numerical experiments

A detailed description of the two-layer eddy-resolving model used for calculations can be found in our previous works [9, 10].

Despite its apparent simplicity, the two-layer model makes it possible to consider the main factors [9] affecting the formation of currents and describes quite well the large-scale circulation features in the upper and lower layers of the Black Sea. These layers are delimited from each other by a permanent pycnocline [11], formed due to freshwater river runoff on the sea surface and penetration into its deep layer of "heavy" salt water through the lower Bosphorus current.

The following parameters were used in the calculations in the model: the spatial resolution (horizontal cell size) $\Delta x = \Delta y = 3000$ m; the time step $\Delta t = 120$ s; the horizontal turbulent viscosity coefficient parameterized by the biharmonic operator, $A_B = 2 \cdot 10^8$ m⁴/s; the bottom friction coefficient proportional to the square of the velocity, $r_H = 0.002$; the coefficient of linear friction between layers $r_L = 2 \cdot 10^{-6}$ m/s; the reduced free fall acceleration 0.032 m/s²; the Coriolis parameter $f = f_0 + \beta y$, where $f_0 = 10^{-4}$ 1/s, $\beta = 2 \cdot 10^{-11}$ 1/s/m; the upper layer thickness at rest $h_0 = 100$ m.

To excite the movement of water masses on the sea surface, a model field of tangential wind stress was set $\tau(x, y, t)$, calculated according to the following formulas:

$$\begin{aligned} \tau_x(x, y, t) &= -\tau_0^x \cos\left(\frac{\pi x}{L} + \pi\left(\frac{1}{2} - \gamma S\right)\right) \cos\left(\frac{\pi y}{B}(1 - S)\right), \\ \tau_y(x, y, t) &= -\tau_0^y \sin\left(\frac{\pi x}{L} + \pi\left(\frac{1}{2} - \gamma S\right)\right) (1 - S) \frac{\left(\frac{x}{\Delta x}\right)^2 + 20000}{\left(\frac{L}{\Delta x}\right)^2 + 20000}, \end{aligned} \quad (1)$$

where τ_0^x, τ_0^y are values constant for each experiment, specifying the maximum value of the tangential wind stress; $\gamma \in [0; 1]$ is the adjusting coefficient that determines the spread of the anticyclonic vorticity zone to the east in summer; L, B are the integration area dimensions along the X and Y axes, respectively; $S = 0.5 \cdot \sin^2(\pi t / 8640)$ is the seasonal course determining parameter; t is the calculation time in hours; Δx is the grid step along the X axis.

Thus, the field $\tau(x, y, t)$ obtained imitates the main features of the real wind effect, namely: the cyclonic nature of the integral vorticity of the tangential wind stress, the seasonal variability of the vorticity τ and the shift of the cyclonic vorticity maximum to the eastern half of the basin [6, 12, 13]. It should be noted that the aforementioned features have an important effect on the large-scale circulation observed in the Black Sea [10].

For a better presentation Fig. 1, *a, b* show the tangential wind stress field used in one of the experiments, obtained by averaging the fields over one year calculated by formula (1), and the vorticity of this average annual field. Fig. 1, *c – e* show the seasonal variability of the wind stress vorticity. It can be seen that in winter, the $\text{rot}_z \tau$ sign over the entire sea corresponds to cyclonic vorticity. Its maximum is in the eastern half of the sea, and in summer, an area of anticyclonic vorticity τ is located over the western part of the sea.

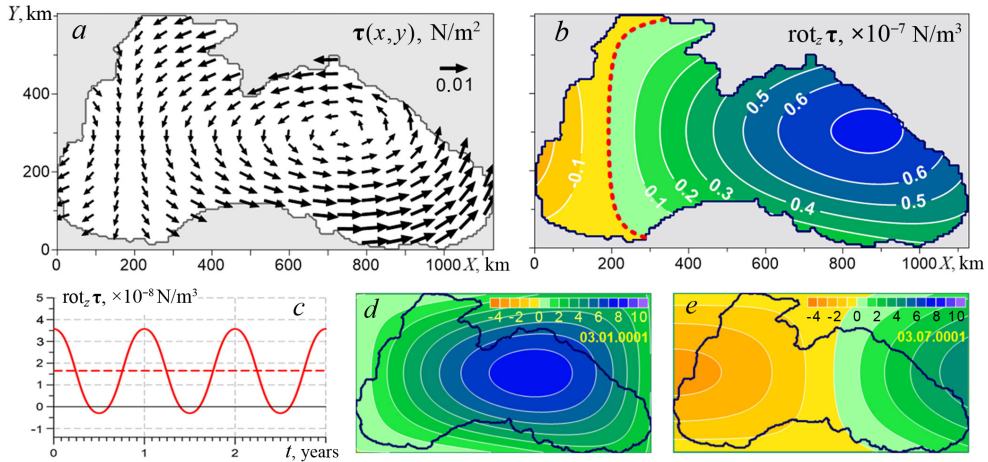


Fig. 1. Annual average fields of the tangential wind stress (*a*) and the tangential wind stress vorticity (*b*); annual variation of the tangential wind stress vorticity average over the water area (*c*) (dashed line corresponds to the annual average value); instantaneous fields of the tangential wind stress vorticity at early January (*d*) and early July (*e*)

In the model version used in this paper, in contrast to previous ones [9, 10], when determining the force of the mechanical effect of the wind on the sea surface, a correction that takes into account the effect of the velocity of surface currents on the tangential wind stress is introduced. The aerodynamic formula for calculating the tangential wind stress [8] in this case takes the following form:

$$\tau^* = \rho_a C_d |\mathbf{U}_a - \mathbf{u}_1| (\mathbf{U}_a - \mathbf{u}_1), \quad (2)$$

where τ^* is the tangential wind stress, taking into account the surface current (N/m^2); ρ_a is the air density (kg/m^3); $C_d = 1.3 \cdot 10^{-3}$ is the empirical dimensionless sea surface drag coefficient; $\mathbf{U}_a = (U_a, V_a)$ is the wind speed at a height of 10 m above the sea (m/s); $\mathbf{u}_1 = (u_1, v_1)$ is the surface current velocity (m/s).

This correction permits to describe the process of momentum exchange between the atmosphere and the sea surface more physically. The papers [14, 15] note the importance of correctly calculating the tangential wind stress acting on the sea surface, since this is the main driving force that forms the currents. The empirical formula for calculating τ does not consider the sea surface movement, the difference in water and air temperatures, which affects the drive stratification of the atmosphere

and the sea surface roughness. These factors can play a big role in the exchange of momentum between the atmosphere and the ocean and influence the simulation results. In this paper, except the other examples, the one is given, when the consideration of surface currents in the calculation of the tangential wind stress affects the final result.

The algorithm for calculating the tangential wind stress at each time integration step is as follows:

– first, using formulas (1), the horizontal components of the tangential wind stress (τ_x, τ_y) at the grid nodes over a still sea are calculated;

– then, using the aerodynamic formula for a fixed surface $\boldsymbol{\tau} = \rho_a C_d |\mathbf{U}_a| \mathbf{U}_a$, the horizontal components of the wind speed at a height of 10 m (U_a, V_a) , corresponding to the shear wind stress calculated above, are determined: from $\boldsymbol{\tau} = \rho_a C_d |\mathbf{U}_a| \mathbf{U}_a$ it follows that $\tau_x = \rho_a C_d |\mathbf{U}_a| U_a$, $\tau_y = \rho_a C_d |\mathbf{U}_a| V_a$, $|\boldsymbol{\tau}| = \rho_a C_d |\mathbf{U}_a|^2$, as a result we obtain

$$U_a = \frac{\tau_x}{\rho_a C_d |\mathbf{U}_a|}, \quad V_a = \frac{\tau_y}{\rho_a C_d |\mathbf{U}_a|}, \quad |\mathbf{U}_a| = \sqrt{\frac{|\boldsymbol{\tau}|}{\rho_a C_d}}, \quad \text{where } |\boldsymbol{\tau}| = \sqrt{\tau_x^2 + \tau_y^2};$$

– after calculating U_a, V_a the horizontal components of the tangential wind stress are recalculated according to formula (2), which takes into account the velocities of surface currents:

$$\begin{aligned} \tau_x^* &= \rho_a C_d |\mathbf{U}_a - \mathbf{u}_1| (U_a - u_1), \\ \tau_y^* &= \rho_a C_d |\mathbf{U}_a - \mathbf{u}_1| (V_a - v_1), \\ |\mathbf{U}_a - \mathbf{u}_1| &= \sqrt{(U_a - u_1)^2 + (V_a - v_1)^2}. \end{aligned}$$

The values τ_x^*, τ_y^* are the components of $\boldsymbol{\tau}^*$, obtained after correction, are used in the model equations. As a result of the correction, the values of $\boldsymbol{\tau}^*$ are smaller than $\boldsymbol{\tau}$, and the vorticity $\boldsymbol{\tau}^*$ is correspondingly smaller.

Time integration in all presented experiments was carried out from a state of rest for a long period, sufficient to consider the obtained solution as statistically equilibrium. This means that when averaging over a certain (large enough) time period, all the average model characteristics should remain constant with a given accuracy. Let us agree to call such a time period statistically equilibrium, or a period of statistical equilibrium.

A series of experiments was carried out, which differed from each other in the intensity of the given field of tangential wind stress $\boldsymbol{\tau}(x, y, t)$. At the same time, the field $\boldsymbol{\tau}(x, y, t)$ variability nature remained unchanged. In each individual experiment, the tangential wind stress had only periodic seasonal variability, and there was no interannual variability. Technically, this consisted in increasing, with a

certain step, of the constant values τ_0^x, τ_0^y used in formulas (1) when passing from the previous experiment to the next. As a wind effect characteristic, the annual and sea area average wind stress vorticity $T = \overline{\langle \text{rot}_z \boldsymbol{\tau}(x, y, t) \rangle}$ was used, which for each individual experiment was a constant value (angle brackets mean spatial averaging, the overline means averaging over time).

As already mentioned, the kinetic energy values in two layers K_1, K_2 and the available potential energy P were chosen as the circulation intensity criterion. The following formulas were used to calculate them:

$$K_1 = \rho_1 \left\langle h_1 \frac{\mathbf{u}_1^2}{2} \right\rangle, \quad K_2 = \rho_2 \left\langle h_2 \frac{\mathbf{u}_2^2}{2} \right\rangle, \quad P = \rho_2 g' \left\langle \frac{(h_1^2 - h_0^2)}{2} \right\rangle,$$

where ρ_1, ρ_2 is the water density in the upper and lower layer; h_1, h_2 are the upper- and lower-layer thickness values; $\mathbf{u}_1, \mathbf{u}_2$ are the current velocities in the layers; h_0 is the upper layer thickness at rest.

In addition to the K_1, K_2, P values, when analyzing the results of experiments, the energy balance components averaged over the sea area were also calculated and analyzed. They are the energy flows, or work per unit time (power) of forces acting on water masses and leading to a change in K_1, K_2, P [16]. The most important flow for the present study is the energy flow from the wind entering the sea (wind pumping) $W_\tau = \rho_1 \langle \boldsymbol{\tau}^* \cdot \mathbf{u}_1 \rangle = \rho_1 \langle |\boldsymbol{\tau}^*| \cdot |\mathbf{u}_1| \cdot \cos(\alpha) \rangle$, where α is the angle between the vectors $\boldsymbol{\tau}^*$ and \mathbf{u}_1 . Since $|\boldsymbol{\tau}^*| \cdot \cos(\alpha) \leq |\boldsymbol{\tau}| \cdot \cos(\alpha)$, it can be stated that the correction introduced in the model leads to a decrease in the energy flow directed from the wind into the sea.

Analysis of the results of numerical experiments

It is convenient to start the analysis with an experiment in which the tangential wind stress field was used with the lowest intensity of all the experiments: the average wind stress vorticity T for the year and for the sea area was $1.5 \cdot 10^{-7} \text{ N/m}^3$. For this experiment Fig. 2 shows the time course graphs of the available potential and kinetic energies averaged over the sea area, as well as the energy flow transferred from the wind to the sea.

When comparing the energy graphs, it is seen that the kinetic energy of the currents in the upper layer K_1 and the available potential energy P correlate well with each other (Fig. 2, *a, b*). The correlation coefficient calculated for these characteristics over a time period of 0–50 years is 0.92, which indicates a strong linear relationship between them. This is a consequence of the quasi-geostrophic nature of large-scale motions and the hydrostatic nature of the model.

The kinetic energy of the currents in the lower layer K_2 takes on values smaller than those of K_1 and P and has a very weak linear correlation with them

(the corresponding correlation coefficients are 0.27 and 0.01). This implies that either K_1 or P can be used to estimate the circulation intensity in the upper layer, while K_2 is better used only to estimate the circulation intensity in the lower layer.

According to Fig. 2, the temporal variability of the energy characteristics of the upper layer in the first experiment includes seasonal variability and significant interannual oscillations with a period of 6–8 years, which are clearly manifested in the frequency spectra of P and K_1 (Fig. 3).

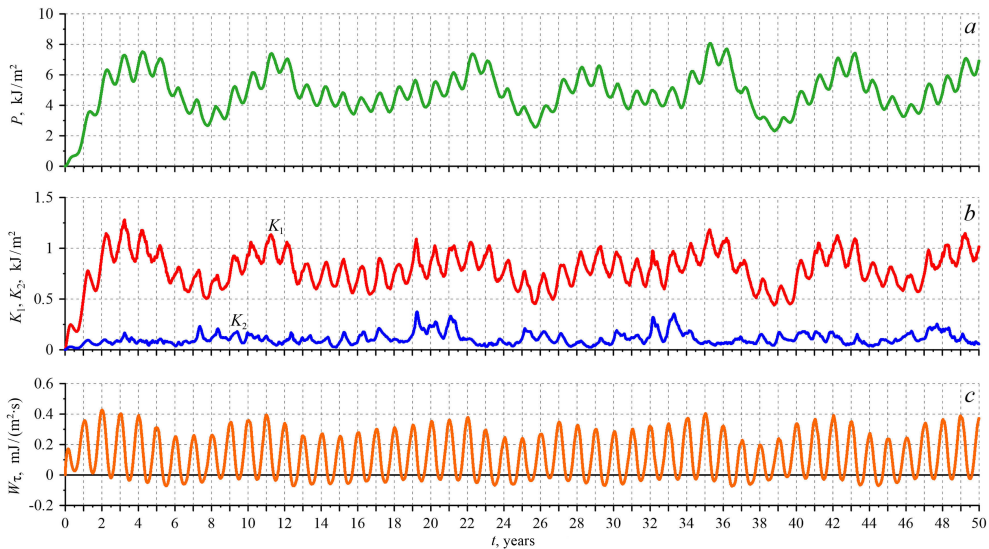


Fig. 2. Temporal variability of the sea area averaged energies P (a), K_1 , K_2 (b), and the wind-induced energy flow W_τ (c)

The seasonal variability of the intensity of the Black Sea currents depending on the tangential stress wind vorticity over the sea is well studied, understandable and does not raise serious issues. In the annual course, the large-scale circulation intensity changes following the energy flow entering the sea from the wind (Fig. 2, c), with a phase lag of about 3 months. This delay is due to the fact that to form gradient currents, the cyclonic wind needs to move large masses of water in the upper layer of the sea towards the coast, and this takes some time. In the experiment under consideration, this time shift was ~ 3 months, or a quarter of the annual period, but it can probably be slightly less or more depending on the external influence characteristics (this issue requires further study).

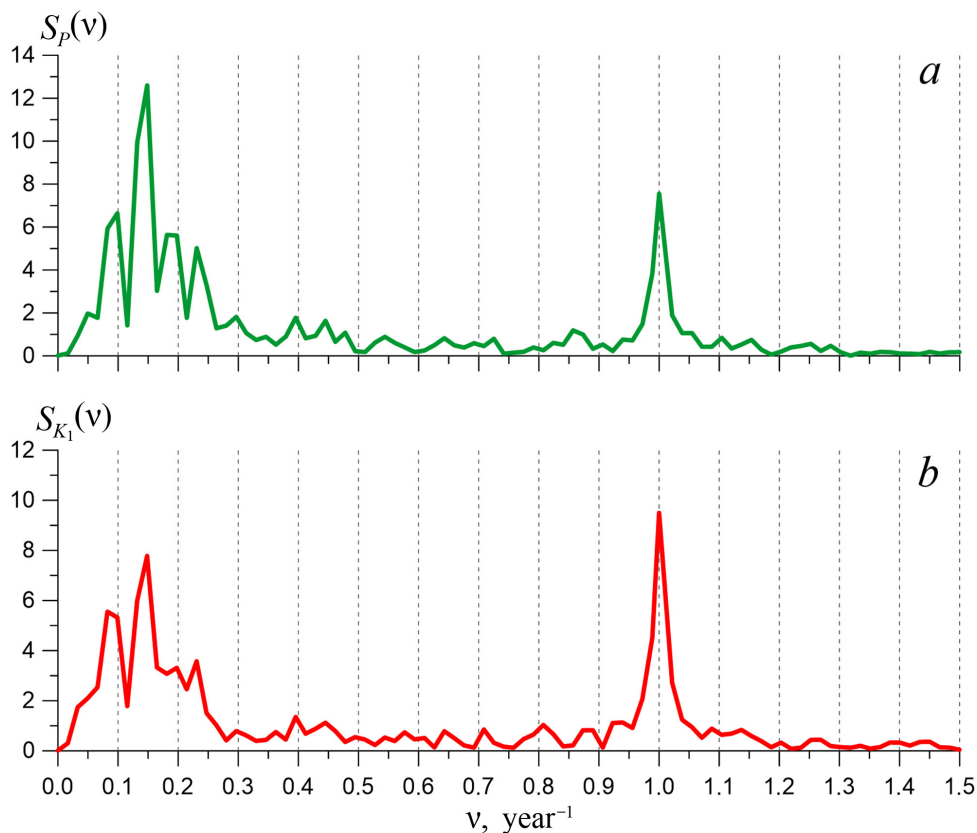


Fig. 3. Frequency spectra of the water area average energies P (a) and K_1 (b)

As for the previously mentioned energy oscillations with a period of several years, their manifestation turned out to be unexpected, given the interannual variability absence of the external wind factor in the model. The latter circumstance gives grounds to classify the interannual variability of circulation intensity obtained in experiments as a self-oscillating process. Self-oscillations are undamped oscillations supported by an external source of energy. Its supply is regulated by the oscillatory system itself¹. When comparing energy oscillations with a change in its inflow from the wind into the sea (Fig. 2), it can be noted that a decrease in the general circulation intensity occurs in years when the wind pumping is reduced. No other reasons for the decrease in energy, such as, for example, an increase in energy dissipation due to bottom friction and/or horizontal turbulent viscosity, have been identified.

Next, we will try to understand the reasons for the wind pumping weakening. The wind energy flow entering the sea is the work per unit time (power) of the wind friction force to move the water mass. As noted above, it is equal to the scalar product of the tangential wind stress and current velocity vectors on the sea surface, and

¹ Kharkevich, A.A., 2009. [*Self-Oscillations*]. Moscow: Librokom, 176 p. (in Russian).

therefore depends on the α angle between these vectors. Since in the experiments under consideration the wind stress fields are set strictly according to formula (1) and do not have interannual variability, only the velocity vectors of surface currents can change from year to year.

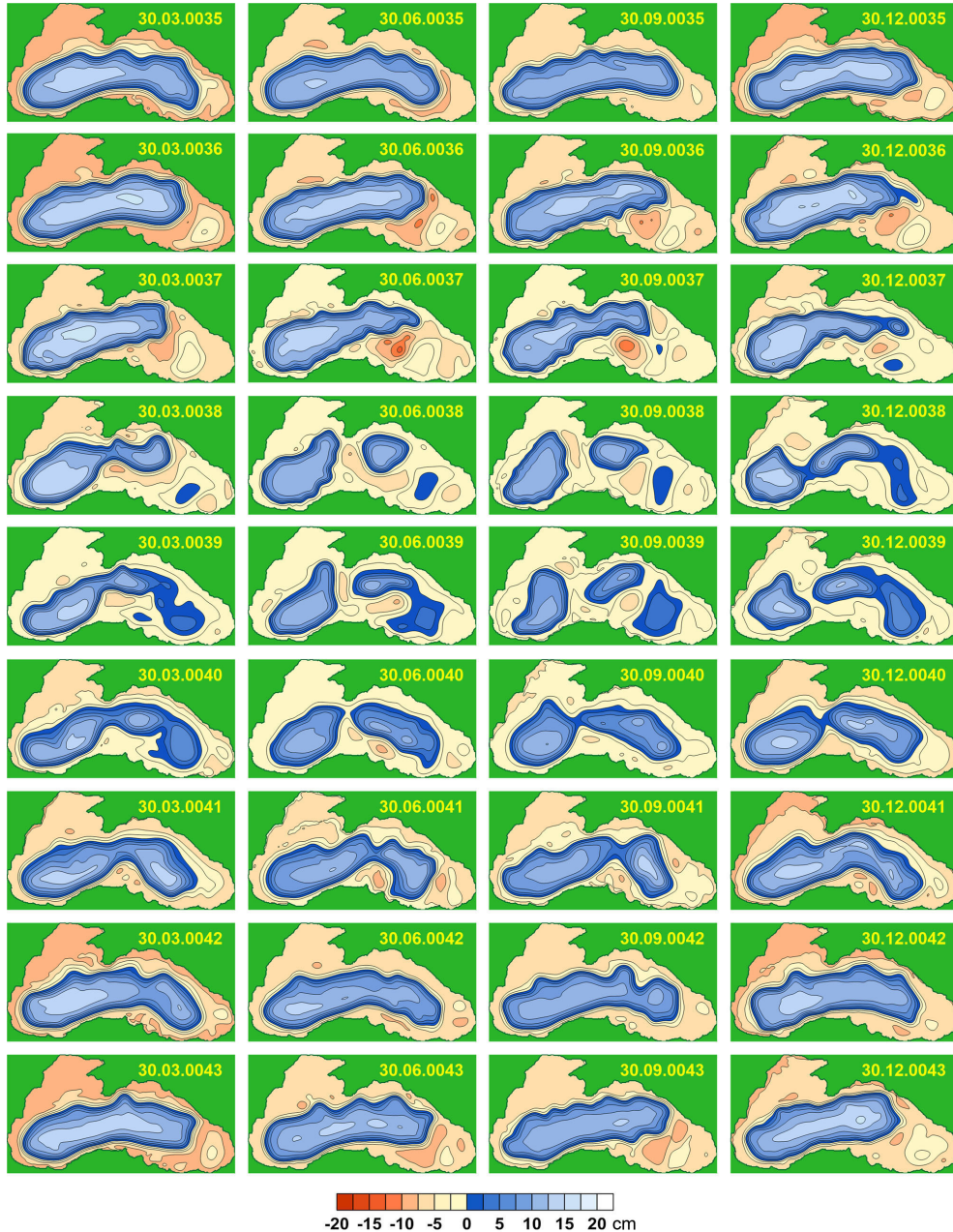


Fig. 4. Successive instantaneous sea level fields ζ (cm) at $T = 1.5 \cdot 10^{-8} \text{ N/m}^3$ (time format – day/month/year)

To understand the circulation variability specifics in the upper layer, let us consider successive sea level maps $\zeta(x, y)$ constructed according to the present experiment data for 9 model years (35–43 years) with a frequency of 3 months (Fig. 4). The selected period corresponds to one complete cycle of the considered fluctuations in energy characteristics (Fig. 2). The spatial distribution of ζ , due to the quasi-geostrophicity of the movements of the considered scales [17], gives a good idea of the upper sea layer currents: the isolines of ζ coincide with current lines, and their thickening corresponds to the position of the Black Sea Rim Current jet.

As a result of a visual analysis of the sea level instantaneous fields, it was found that in the years with maximum energy flow from the wind into the sea, the large-scale circulation was one large Rim Current cyclonic gyre, which was most widespread over the sea area (Fig. 4, year 35). A similar circulation in the experiment under consideration was formed in the years 4, 11, 22, 35 and 42. A large energy inflow leads to an even greater intensification of currents (Fig. 4, 30.03.0036); therefore, in the years at the beginning of which W_τ was maximum, the largest P , K_1 values were noted. Thus, there is a positive feedback between the intensity of circulation and the energy inflow from the wind. In the version of the model used, this feedback has a limitation due to the tangential wind stress correction, as a result of which the velocity of the surface current cannot exceed the wind speed that this current causes.

In the years with the maximum energy inflow (in the cycle under consideration, this is year 35), in the summer period, the Rim Current jet, located above the continental slope in the eastern part of the sea, moved away from the coast and began to move westward at a speed of $\sim 0.5\text{--}0.8$ cm/s, which led to compression of the Rim Current large-scale circulation from the eastern side and its displacement to the western part of the basin. This process continued in the autumn-winter period of the year 35 and further – throughout year 36. The movement of the Rim Current jet in the eastern part of the sea led to a mismatch between the fields τ and \mathbf{u}_1 and, as a result, to a decrease in the wind energy inflow into the sea, which in turn contributed to a circulation intensity decrease.

The described mechanism provides the negative feedback necessary for the existence of self-oscillations. The moving Rim Current jet velocity from east to west corresponds to the phase velocity of the first mode of the baroclinic Rossby wave [18], which, for a two-layer fluid, can be calculated by the formula $C_R = -\beta R_1^2 = -\beta(\sqrt{g'h_0}/f_0)^2$, where R_1 is the baroclinic radius of Rossby deformation. Taking into account the parameter values specified in the model, $C_R = -0.64$ cm/s, which is quite consistent with the results obtained.

During year 37, the cyclonic circulation was further compressed into the western part of the basin and the large-scale circulation intensity decreased. But already in the winter of years 37–38 and in the spring of year 38, signs of a new (still weak) cyclonic circulation formation appeared in the eastern part of the basin, which broke up into several separate cyclonic eddies in the summer and autumn of year 38. In the next 39–41 years, new large-scale currents formed in the basin against the

background of a weakened cyclonic circulation in the western part of the sea that remained from the previous circulation. A characteristic feature of the circulation in these years was its division in the summer period into separate large-scale cyclones - "Knipovich spectacles".

In March of year 42, the Rim Current cyclonic circulation reached its maximum distribution, as in year 35, and then the current transformation cycle was repeated.

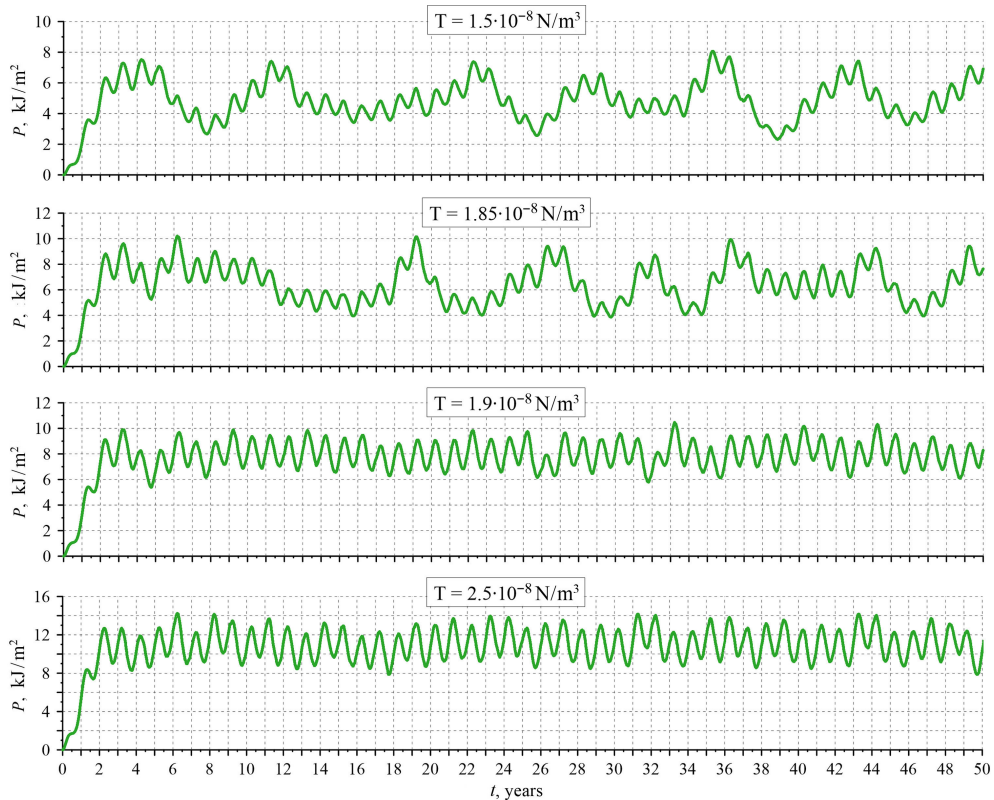


Fig. 5. Change in the sea area averaged available potential energy in the experiments at different values T

In the work of G. F. Safronov ² devoted to the study of the influence of wind action on a two-layer fluid, it was shown that the seasonal variability of the external wind action in a two-layer sea should lead to hydrodynamic instability of a large-scale current and the formation of baroclinic Rossby waves near the eastern coast of the sea. It can be assumed that the Rim Current jet separation from the eastern coast in years with maximum circulation intensity is the result of such a process. It should be noted that Rossby waves were also formed in the basin in other years, but in the absence of a strong Rim Current branch near the eastern coast, the velocity field

² Safronov, G.F., 1985. [*Excitation of Long Waves in the Ocean by Large-Scale Changes in the Tangential Stress Field of the Wind*]. Moscow: Gidrometeoizdat, 108 p. (in Russian).

change in the upper layer of the sea during the passage of these waves did not lead to a sharp decrease in W_{τ} .

In the following experiments, with a successive increase in the tangential wind stress intensity and an increase in its average vorticity to a value of $T = 1.85 \cdot 10^{-8} \text{ N/m}^3$, there were no significant changes of the large-scale circulation inherent for the first experiment (Fig. 4). Only a proportional to T increase in the values of the energy characteristics was observed (Fig. 5, *a, b*). But at T equal to $1.90 \cdot 10^{-8} \text{ N/m}^3$ and more, the previously obtained oscillations in the large-scale circulation intensity ceased to manifest, only its seasonal changes remained, at which the circulation intensified in the winter and spring seasons, and in summer due to the aggravation of hydrodynamic instability of currents as the wind pumping weakened, the Rim Current meandering became more active (Fig. 5, *c, d*).

The absence of generation of long-term oscillations in the energy of currents at large values of T can be explained by the termination of the Rim Current jet separation and movement in the east of the basin during summer periods (Fig. 6), which disabled the feedback mechanism described above, leading to a decrease in the W_{τ} flow.

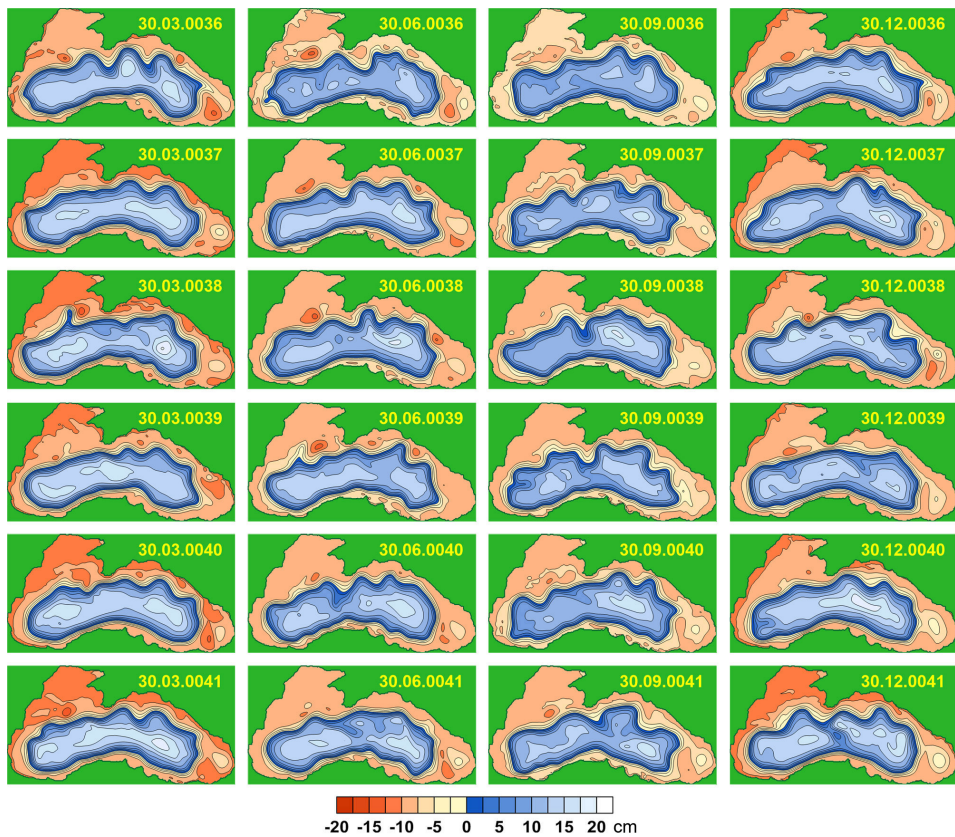


Fig. 6. Successive instantaneous sea level fields ζ (cm) at $T = 1.90 \cdot 10^{-8} \text{ N/m}^3$ (time format – day/month/year)

The simplest explanation of the reason for the Rim Current stabilization with an increase in wind action is that there is simply not enough time for the Rossby wave formation in the form of current separation from the eastern slope of the basin with a $\text{rot}_z \tau$ decrease in summer. Fig. 6 shows that in the summer months, the Rim Current jet in the east of the sea begins to move westward, but the strengthening of the wind stress vorticity in autumn and winter returns the Rim Current to its original place.

Another possible reason of why the Rossby wave does not appear and the Rim Current eastern jet position is preserved can be more powerful currents that form in the lower sea layer due to a stronger wind stress vorticity. During the summer weakening of wind pumping, these currents are able to maintain P and K_1 . According to the potential eddy conservation law, the currents in the lower layer are forced to follow along the isobaths and the baroclinic Rossby wave is not powerful enough to tear them away from the continental slope.

The presented features of the formation of currents under the action of a periodic wind are in some sense consistent with the laboratory modeling results [6] on studying the response of the steady motion of a two-layer fluid in a rotating basin to the external wind action variability. In laboratory experiments, when the wind action ceased for a short period of time, followed by its resumption, the general circular circulation in the basin was restored. If the time interval with the “turned off” wind increased, then after its resumption, the previous circulation was not restored, but broke up into separate eddies moving to the basin center. At the same time, a new large-scale circulation was forming along the coast. In the numerical experiments considered in this paper, it was not the duration of the wind effect that changed, but its average intensity. However, the results obtained are similar: two flow regimes were also obtained with the restoration of the old circulation and the formation of a new one.

Conclusion

The carried-out numerical experiments have shown that when the sea surface is exposed to a periodic seasonally changing wind in the Black Sea, depending on the value of the average annual wind stress vorticity, two modes of large-scale circulation are possible.

The first one can exist at small values of the average annual tangential wind stress vorticity. This regime is characterized by the presence of significant interannual variability of the circulation intensity in the form of oscillations with a period of 6–8 years. In essence, such oscillations are self-oscillations, in which the key that provides feedback is the dependence of the wind energy flow entering the sea on the change in the Rim Current jet position, caused by the baroclinic Rossby wave formation near the eastern boundary and further movement to the west. Seasonal variability of external wind conditions contributes to the annual formation of such waves. However, the Rossby waves have a significant impact on the energy flow coming from the wind into the sea only if a powerful Rim Current flow in the eastern part of the sea falls under their influence.

In the present paper, it is established that for the existence of circulation intensity self-oscillations, it is necessary that the average value of the tangential wind stress

curl T for the year and for the sea area does not exceed a certain threshold value, which in the presented calculations was $1.85 \cdot 10^{-8} \text{ N/m}^3$.

At T equal to $1.90 \cdot 10^{-8} \text{ N/m}^3$ and more, another circulation regime was formed, in which the above self-oscillations did not form, and the large-scale circulation intensity was determined by the magnitude of the tangential wind stress vorticity. Energy oscillations in this case had only a seasonal course, and the limitation of the energy flow into the sea was due to the Rim Current meandering, which intensified in summer.

The observed value of the average annual wind stress vorticity over the Black Sea is $1.67 \cdot 10^{-8} \text{ N/m}^3$, which is less than the above threshold value. Consequently, long-term oscillations in the circulation intensity due to the internal dynamics of the sea can be present in the observational data with a high probability. Let us note that the use of a correction in the wind stress calculation led to a significant increase in the threshold value for the wind stress vorticity, below which self-oscillations of the circulation intensity occurred in the model. Without correction, the threshold value T would be equal to $\sim 1.20 \cdot 10^{-8} \text{ N/m}^3$ and the above self-oscillations existence in the Black Sea would be considered unlikely.

The principal conclusion of this paper is that, in addition to changes in the tangential wind stress and its average vorticity over the water area, the intensity of large-scale circulation in the Black Sea can be significantly affected by hydrodynamic processes in the upper sea layer caused by seasonal variability of wind conditions over the sea surface.

REFERENCES

1. Korotaev, G.K., 2001. On a Reason of Seasonal Variation of the Black Sea Circulation. *Morskoy Gidrofizicheskiy Zhurnal*, (6), pp. 14-20 (in Russian).
2. Stanev, E.V., 2005. Understanding Black Sea Dynamics: Overview of Recent Numerical Modeling. *Oceanography*, 18(2), pp. 56-75. doi:10.5670/oceanog.2005.42
3. Polonsky, A.B. and Shokurova, I.G., 2010. Variations of the Seasonal Behavior of Geostrophic Circulation in the Black Sea. *Physical Oceanography*, 20(1), pp. 14-27. doi:10.1007/s11110-010-9064-4
4. Knysh, V.V., Korotaev, G.K., Moiseenko, V.A., Kubryakov, A.I., Belokopytov, V.N. and Inyushina, N.V., 2011. Seasonal and Interannual Variability of Black Sea Hydrophysical Fields Reconstructed from 1971–1993 Reanalysis Data. *Izvestiya, Atmospheric and Oceanic Physics*, 47(3), pp. 399-411. doi:10.1134/S000143381103008X
5. Korotaev, G.K., Sarkisyan, A.S., Knysh, V.V. and Lishaev, P.N., 2016. Reanalysis of Seasonal and Interannual Variability of Black Sea Fields for 1993–2012. *Izvestiya, Atmospheric and Oceanic Physics*, 52(4), pp. 418-430. doi:10.1134/S0001433816040071
6. Zatsepin, A.G., Kremenetskiy, V.V., Stanichny, S.V. and Burdyugov, V.M., 2010. Black Sea Basin-Scale Circulation and Mesoscale Dynamics under Wind Forcing. In: A. V. Frolov and Yu. D. Resnyansky, eds., 2010. *Modern Problems of Ocean and*

Atmosphere Dynamics. The Pavel S. Lineykin Memorial Volume. Moscow: TRIADA LTD., pp. 347-368 (in Russian).

7. Polonsky, A.B. and Shokurova, I.G., 2011. Long-Term Variability of the Tangential Wind Stress Vorticity over the Black Sea from the Reanalysis Data. In: MHI, 2011. *Ekologicheskaya Bezopasnost' Pribrezhnoy i Shel'fovoy Zon Morya* [Ecological Safety of Coastal and Shelf Zones and Comprehensive Use of Shelf Resources]. Sevastopol: MHI. Iss. 24, pp. 182-189 (in Russian).
8. Shokurov, M.V. and Shokurova, I.G., 2017. Wind Stress Curl over the Black Sea under Different Wind Regimes. *Physical Oceanography*, (6), pp. 12-23. doi:10.22449/1573-160X-2017-6-12-23
9. Pavlushin, A.A., 2018. Numerical Modeling of the Large-Scale Circulation and Mesoscale Eddies in the Black Sea. In: SOI, 2018. *SOI Proceedings*. Moscow: SOI. Iss. 219, pp. 174-194 (in Russian).
10. Pavlushin, A.A., Shapiro, N.B., and Mikhailova, E.N., 2018. Influence of Seasonal Variability of the Wind Stress Vorticity on the Structure of the Black Sea Circulation. *Physical Oceanography*, 25(5), pp. 345-358. doi:10.22449/1573-160X-2018-5-345-358
11. Ivanov, V.A. and Belokopytov, V.N., 2013. *Oceanography of the Black Sea*. Sevastopol: ECOSY-Gidrofizika, 210 p. (in Russian).
12. Efimov, V.V. and Anisimov, A.E., 2011. Climatic Parameters of Wind-Field Variability in the Black Sea Region: Numerical Reanalysis of Regional Atmospheric Circulation. *Izvestiya, Atmospheric and Oceanic Physics*, 47(3), pp. 350-361. doi:10.1134/S0001433811030030
13. Efimov, V.V. and Yurovsky, A.V., 2017. Formation of Vorticity of the Wind Speed Field in the Atmosphere over the Black Sea. *Physical Oceanography*, (6), pp. 3-11. doi:10.22449/1573-160X-2017-6-3-11
14. Ferrari, R. and Wunsch, C., 2009. Ocean Circulation Kinetic Energy: Reservoirs, Sources, and Sinks. *Annual Review of Fluid Mechanics*, 41(1), pp. 253-282. doi:10.1146/ANNUREV.FLUID.40.111406.102139
15. Renault, L., Molemaker, M.J., McWilliams, J.C., Shchepetkin, A.F., Lemarié, F., Chelton, D., Illig, S. and Hall, A., 2016. Modulation of Wind Work by Oceanic Current Interaction with the Atmosphere. *Journal of Physical Oceanography*, 46(6), pp. 1685-1704. doi:10.1175/JPO-D-15-0232.1
16. Pavlushin, A.A., Shapiro, N.B., and Mikhailova, E.N., 2019. Energy Transitions in the Two-Layer Eddy-Resolving Model of the Black Sea. *Physical Oceanography*, 26(3), pp. 185-201. doi:10.22449/1573-160X-2019-3-185-201
17. Kantha, L.H. and Clayson, C.A., eds., 2000. *Numerical Models of Oceans and Oceanic Processes. International Geophysics, vol. 66*. California, USA: Academic Press, 940 p. doi:10.1016/s0074-6142(00)x8001-1
18. Belonenko, T.V., Foux, V.R., and Koldunov, V.V., 2012. On Standing-Progressive Rossby Waves in Sea and Ocean. *Vestnik Vestnik of Saint-Petersburg University. Geology. Geography*, (2), pp. 91-103 (in Russian).

About the author:

Andrey A. Pavlushin, Junior Research Associate, Marine Hydrophysical Institute of RAS (2 Kapitanskaya Str., Sevastopol, 299011, Russian Federation), **ResearcherID: R-4908-2018**, pavlushin@mhi-ras.ru

The author has read and approved the final manuscript.

The author declares that he has no conflict of interest.